

Flow over Double-Delta Wing and Wing Body at High α

David Manor*

Parks College, Cahokia, Illinois

and

William H. Wentz Jr.†

Wichita State University, Wichita, Kansas

The effects of sideslip on the performance and stability of a double-delta wing and wing-body configuration were determined experimentally. The wake total pressure reveals the vortex size, location, and shape. Sideslip angle resulted in a decreased stall angle of attack, lower $C_{L_{MAX}}$, enhancement of post-stall lift recovery, increased upwind vortex sheet size, and decreased downwind vortex size. Adding the body to the wing increased the levels of adverse rolling and yawing moments at the stall. The wake surveys show that a narrow band at the edge of the vortex sheet has a very steep total pressure gradient present in all configurations.

Nomenclature

A	= wing aspect ratio, 1.6
b	= wing span
c_0	= wing root chord
\bar{c}	= wing mean chord, 47.67 cm
C_D	= drag coefficient, $D/(q_\infty S)$
C_L	= lift coefficient, $L/(q_\infty S)$
$C_{L\beta}$	= $dC_L/d\beta$
$c_{n\beta}$	= $d(C_n)/d\beta$
C_M	= pitching moment coefficient, $M/(q_\infty S\bar{c})$
C_{P_t}	= total pressure coefficient, $(P_t - P_{S_\infty})/q_\infty$
C_n	= yawing moment coefficient, $N/(q_\infty Sb)$
C_r	= rolling moment coefficient, $L'/(q_\infty Sb)$
C_y	= side force coefficient, $Y/q_\infty S$
d	= diameter
d_n	= nose diameter
D	= drag force
L	= lift force
l	= body length
l_n	= nose length
M	= pitching moment
L'	= rolling moment
N	= yawing moment
Y	= sideforce
P_t	= local total pressure
P_{S_∞}	= freestream static pressure
q_∞	= freestream dynamic pressure
R_e	= Reynolds number, $U\bar{c}/\nu$
S	= wing reference area, 0.1612 m ²
V_∞	= freestream velocity
x	= coordinate parallel to wing chord
α	= geometric angle of attack
β	= sideslip angle
Λ	= wing leading-edge sweep angle
ν	= kinematic viscosity

Subscripts

s	= static
t	= total

Received May 29, 1984; revision received Aug. 8, 1984. Copyright © American Institute of Aeronautics and Astronautics, Inc., 1984. All rights reserved.

*Assistant Professor, Dept. of Aerospace Engineering and Engineering Sciences. Member AIAA.

†Professor, Dept. of Aeronautical Engineering. Associate Fellow AIAA.

w	= wing
wb	= wing body
∞	= freestream value

Introduction

ERODYNAMICS of highly swept fighter configurations are dominated by vortex flows. At sideslip angles other than zero, the vortex formation over delta wings is asymmetric and may affect aircraft stability. At high angles of attack, vortex bursting occurs. Vortex bursting (breakdown of the stable, spiral structure) is due to the instability emanating from the core outward. The bursting location moves progressively toward the apex as the angle of attack increases. When bursting is symmetric, only pitch stability is affected, i.e., as the bursting location moves toward the apex, the distribution of lift is such that a pitch-up results. If vortex bursting is asymmetric, a rolling moment will also result, adversely affecting roll and yaw stability.

Because vortex bursting on a low sweep wing occurs at lower angle of attack, it causes roll into the sideslip direction if differential bursting occurs ($C_{L\beta} < 0$) since the effective sweep is reduced on the upwind side of the wing and increases on the downwind side. If a body is present (e.g., fuselage) a pair of vortices is shed from the body and an additional side force is produced due to the flow around the body, resulting in a net side force which usually tends to cause a yaw in the opposite direction to sideslip ($C_{n\beta} < 0$). This phenomenon is known by fighter pilots as "nose slice" and may cause the aircraft to go into a spin. For highly swept wings, the two vortex sheets formed over the wing may make contact (i.e., roll on top of one another) and may also cause asymmetries, thereby adversely affecting stability.

The flow over double-delta wings, although similar to that of simple deltas, is much more complex. At low angles of attack ($\alpha < 10$ deg), two primary vortices are shed on each side of the wing, one from the apex and the other from the break in the wing. The vortex shed from the apex (known as the inner vortex) follows a line roughly parallel to the upper delta sweep. The vortex shed from the break (known as the outer vortex) follows a line parallel to the leading edge. Two secondary vortices may accompany these vortices. At higher angles of attack ($\alpha > 10$ deg), the two primary vortices merge (or join) and follow a line parallel to the leading edge, that is, the weaker inner primary vortex and the stronger outer vortex intertwine and follow the path of the stronger outer vortex.¹⁻⁸

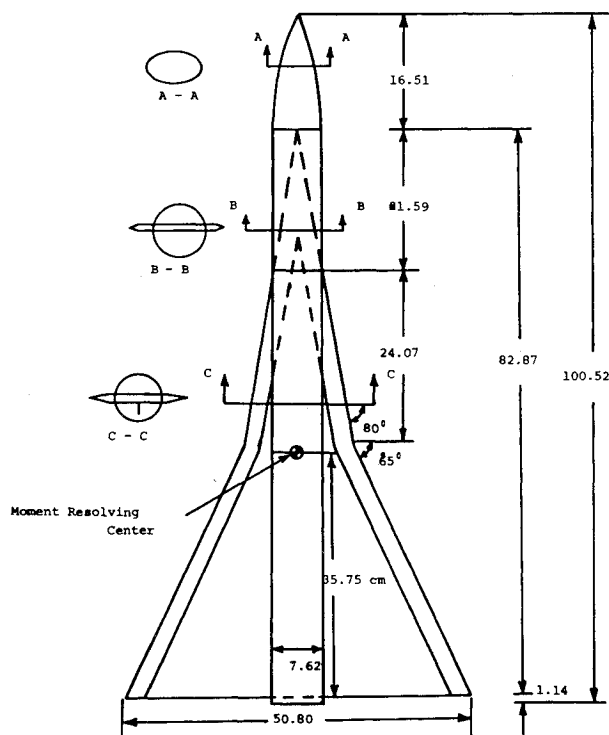


Fig. 1 Model.

Since most of previous double-delta flow work at high angles of attack was done with the accent on wing-alone configurations (e.g., Refs. 9-12), the present research goal is to investigate wing-body combinations.

Experimental Investigation

Test Apparatus and Model Description

All tests were conducted in the Walter H. Beech Wind Tunnel. This is a closed-return, low-speed wind tunnel with a 213×305 cm (7×10 ft) test section that operates at atmospheric pressure. Most tests were conducted at a dynamic pressure of 718 Pa (15 psf) corresponding to a Mach number of 0.10 and Reynolds number of 1.2×10^6 (based on mean chord).

The wing model used in this research is one of the models used in Ref. 12. A cylindrical fuselage and an elliptical nose were fitted to the model. The shapes and dimensions are given in Fig. 1.

Wake total pressure surveys were made using special scanning and signal detectors and indicator apparatus that was developed by Ostowari.¹³ This equipment is similar to a device developed at the Boeing Company.¹⁴ The pressure probe apparatus activates a series of light-emitting diodes (LEDs) based on preset total pressure levels relative to the freestream. The light emitted by the LEDs was sufficient for a color positive ASA 400 film. The camera shutter was kept open during the test period and the tunnel was completely darkened except for the LED illumination. The slides of the wake and a low-light model image were later superimposed in the photo lab.

The wake total pressure surveys were done in the latter part of this work. It was necessary to choose one angle of attack at which to perform the wake surveys. Dr. J. E. Lamar, suggested that these surveys should be made at an angle of attack below the stall in order to determine the effect of sideslip on the configurations tested at high angle-of-attack prestall condition. Since the wing-body configuration was found to stall at $\alpha = 32$ deg with zero sideslip and at $\alpha = 28$ deg and at $\beta = -4$ deg, it was decided to perform the wake surveys at $\alpha = 26$ deg with $\beta = 0$ deg and ± 4 deg. It was felt that these

Table 1 Color code vs pressure level

LED color	Pressure level
Red	$C_{P_t} < 0.01$
Yellow	$0.50 > C_{P_t} > 0.01$
Green	$0.95 > C_{P_t} > 0.50$
Black (no color)	$C_{P_t} > 0.95$

angles would ensure flow data at large angles just below stall for all configurations.

As was mentioned earlier, the wake total-pressure surveys were made with a special apparatus developed at Wichita State University. These surveys were recorded on a color-positive film through a camera placed 9 m (18 spans) downstream from the trailing edge of the model. The end result was a color slide of total pressure isobars of the wake for each configuration. There were three preset wake pressure levels which were translated into color codes as shown in Table 1.

Negative black-and-white transparencies were made from the color slides. The negatives of the model and the wake were superimposed and printed from these. The only drawback to this procedure was that the green band could not be seen on the black-and-white reproduction. This green band, however, is extremely narrow and could be seen by projection of the original color slides. The results of this study are given in Figs. 2 and 3. Figures 2 and 3 were achieved by enlarging the negatives and superimposing them in an isometric view. The photographs depict the rolled sheet (white) and the core in the middle (gray). It was found that at $\beta = \pm 4$ deg, the vortex sheet of the wing and the wing-body configurations are mirror images. For that reason it is believed that probe interference is minimal and only $\beta = -4$ deg isometric view is given (Fig. 3).

Results and Discussion

Wake Survey Data

The wake-total-pressure surveys (Figs. 2 and 3) were obtained by superimposing wake color prints and the model at the stations surveyed. These sketches depict the "true" picture of the wake and are directly proportional to the wing size. The flow sketches indicate that at $\beta = 0$ (Fig. 2), the vortex sheets are initially in contact over the wing and the wing-body and are asymmetric. At $x/c_0 = 0.74$, the two primary vortices have merged. At the trailing-edge ($x/c_0 = 1.00$), the vortices are distinctly separate and appear symmetric. There is evidence of a trapped region of freestream stagnation pressure (white) inside the vortices over the wing. At $x/c_0 = 1.67$, the vortices are further apart and appear symmetric.

At $\beta = -4$ (Fig. 3), the asymmetries are larger and the vortices are blown downwind. The vortex core from the upwind wing panel increases in size relative to that of the downwind side because of the change in effective sweep between the upwind and the downwind wing panels. This relative enlargement is particularly evident at $x/c_0 = 1.67$. Since vortex bursting at this angle of attack (26 deg) is behind the trailing edge, it appears that the vortex sheet enlarges prior to bursting. The vortex sheet expansion downstream is much larger for the wing-body configuration. The spacing of the vortices is further apart for the wing-body configuration.

The wake surveys also revealed a narrow band of steep total pressure gradient at the outer edge of the vortex sheet for all conditions. This pressure gradient is a result of high circumferential velocity at the outer perimeter of the vortex sheet. The interior gradients are not as steep. The enlargement of the upwind vortex relative to the downwind vortex with sideslip indicates the change in the position, shape, and total pressure coefficient of the vortices at large prestall angles. The resulting flow sketches clearly show the trend of viscous region enlargement leading toward vortex bursting.

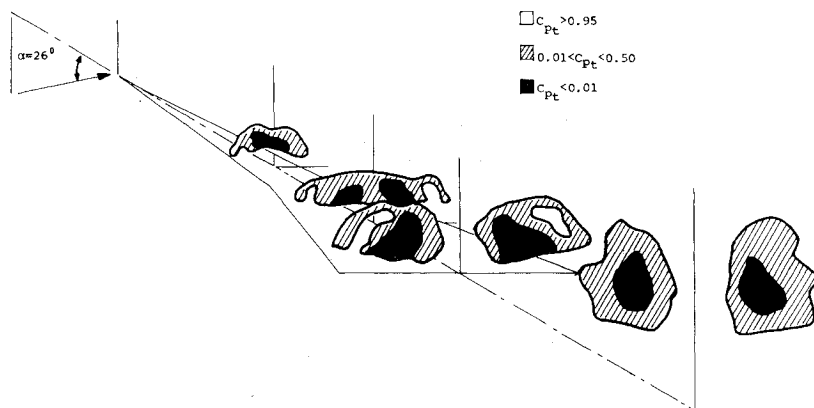


Fig. 2a Wake total pressure surveys; $\beta = 0$ deg, $\alpha = 26$ deg, wing.

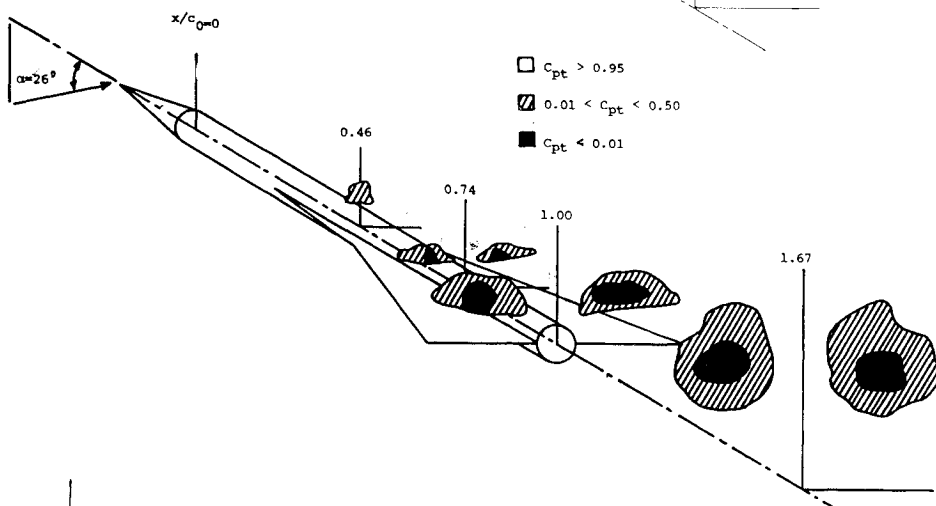


Fig. 2b Wake total pressure surveys; $\beta = 0$ deg, $\alpha = 26$ deg, wing body.

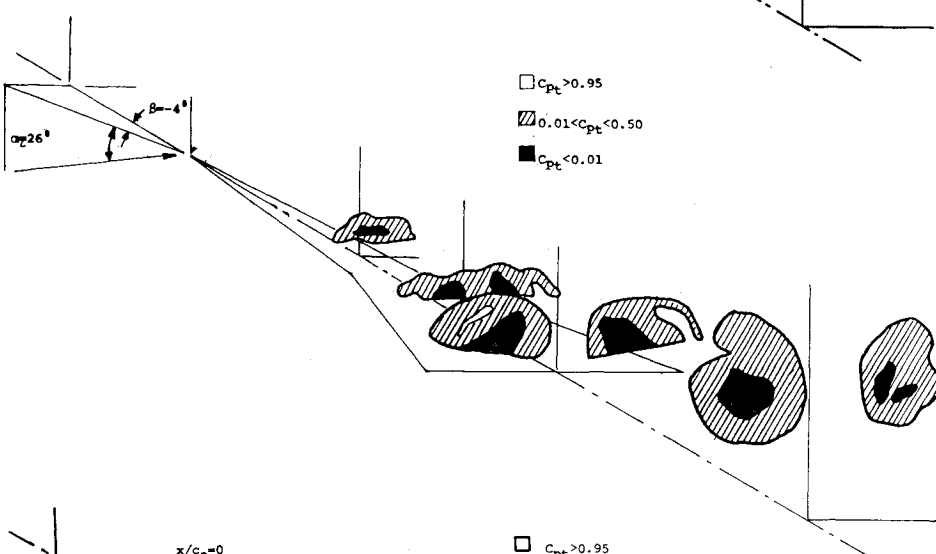


Fig. 3a Wake total pressure surveys; $\beta = 4$ deg, $\alpha = 26$ deg, wing.

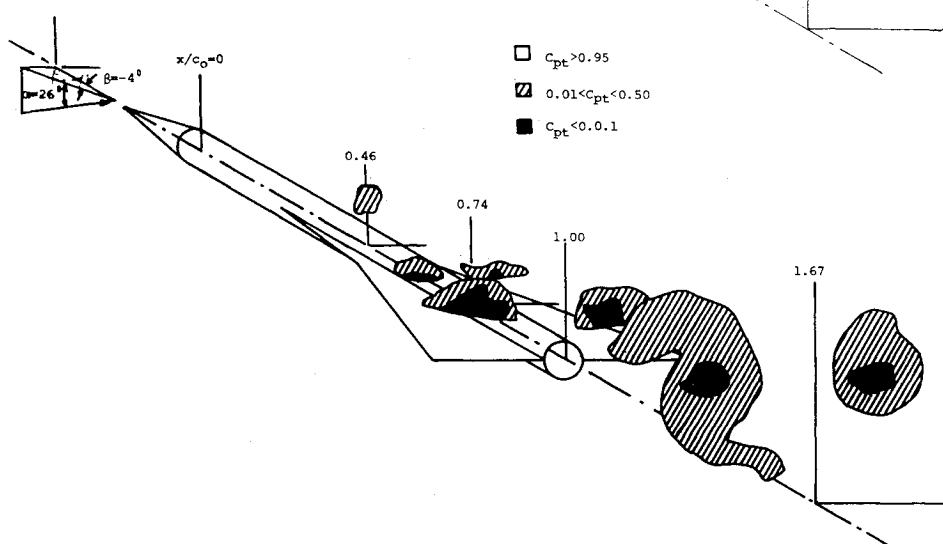


Fig. 3b Wake total pressure surveys; $\beta = 4$ deg, $\alpha = 26$ deg, wing body.

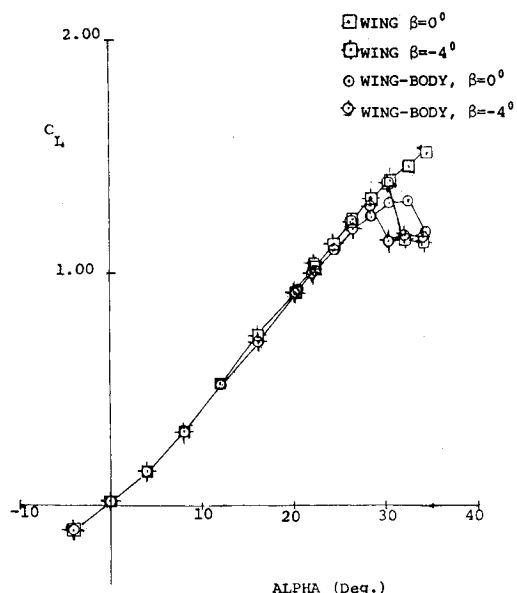


Fig. 4a Measured forces and moments, lift.

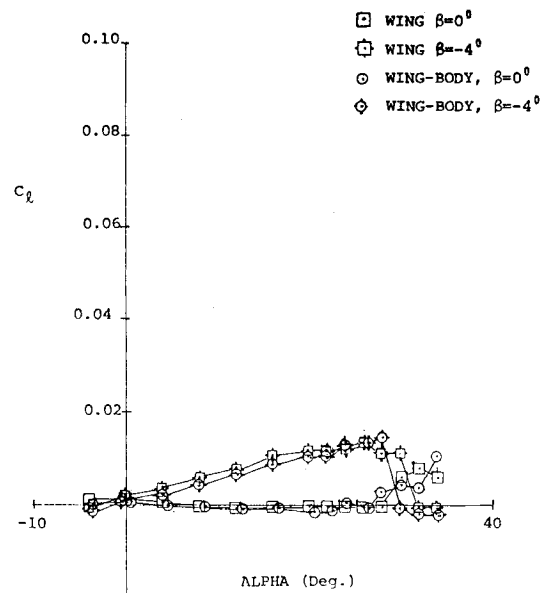


Fig. 4d Measured forces and moments, roll.

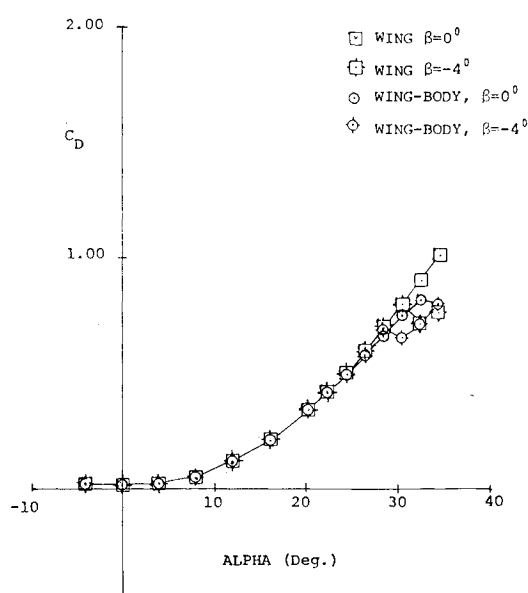


Fig. 4b Measured forces and moments, drag.

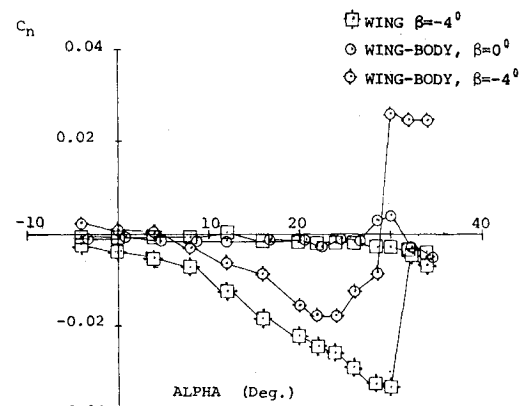


Fig. 4e Measured forces and moments, yaw.

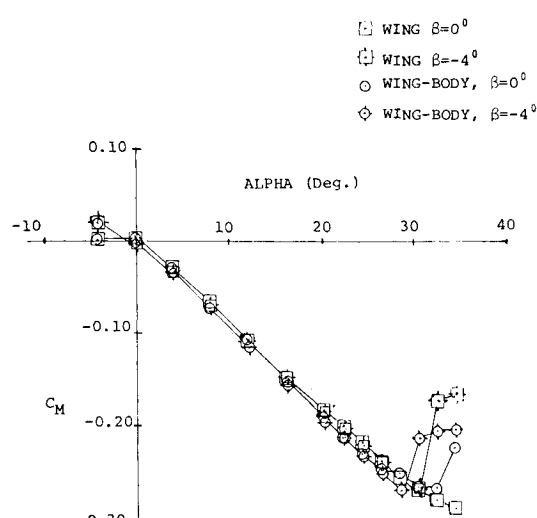


Fig. 4c Measured forces and moments, pitch.

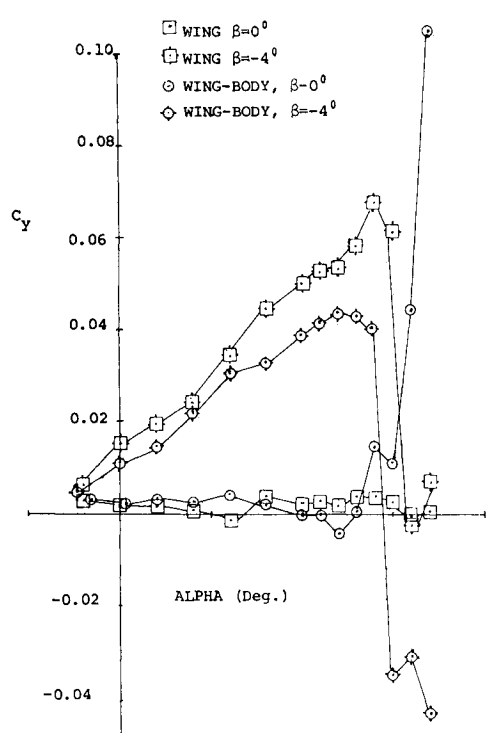


Fig. 4f Measured forces and moments, sideforce.

Force Data

Even though both wing and body when tested alone produced positive lift, the addition of the body to the wing results in a reduction in lift, and the post-stall lift reduction is delayed with sideslip. In fact, there is a post-stall lift recovery after the initial stall $30^\circ \leq \alpha \leq 44^\circ$ (Fig. 4).

The large viscous region in the flow of the wing-body configuration indicates susceptibility to bursting, which is consistent with the wind tunnel force data. The wing-body configuration stalls 2 deg earlier than the wing alone. Wing-body interference reduces $C_{L\text{MAX}}$ by 0.35 at $\beta = 0$ deg, and by 0.20 at $\beta = -4$ deg; C_D is reduced by the same amount at the maximum lift coefficient.

The effects of the merging of the primary vortices on the wing alone were observed previously by Brennenstuhl and Hummel¹¹ at zero sideslip. The present research includes the effect of merging with nonzero sideslip on the lateral and longitudinal stability of the wing and wing body. In pitch, both wing and wing body are stable up to the stall angle (Fig. 4c) with the wing body having a slightly greater stability level.

Vortex merging for the wing is completed at $\alpha = 16$ deg; for the wing body it is complete at $\alpha = 12$ deg. This merging may account for some of the added pitch stability associated with the wing-body configuration; however, it should be noted that the body covers the wing apex and reduces the front panel where the vortex sheets make contact over the wing. This reduction in the front panel area, particularly of the apex, also helps to account for the added pitch stability since wing vortex formation is farther downstream with the wing-body configuration. The merging causes a change in sideforce slope (as well as reducing the values of the maximum pitch and lift) due to the displacement of the vortices in sideslip. In turn, the merging causes a change in the yawing moment slope.

The destabilizing effect of the forebody on the wing-body configuration in the lateral plane can be seen in the lateral force data and the wake surveys. The body vortices were stable in an asymmetric condition. As reported earlier by Moore et al.,¹⁵ the main effect of the forebody is to enhance departures at high angles due to asymmetric vortex formations over the forebody. The wake survey pictures suggest that the forebody (nose) vortices have merged with the wing vortices behind the break in the wing.

The spacing of the vortices farther apart due to the presence of the body will be expected to cause large out-of-plane forces and moments when asymmetric bursting occurs. This is clearly shown in Fig. 4 where the change in lateral forces and moments for the wing body near the stall is larger than the wing alone configuration. This is particularly evident in the yawing moment and sideforce data. These large increments may lead to departures and loss of control followed by a pilot bailout.

Conclusions

The effects of large angles of pitch with 4 deg sideslip on the performance and stability of double-delta wing and wing-body configurations were determined experimentally using six-component force measurements and wake total pressure surveys.

The effect of sideslip was to 1) decrease the stall angle of attack, 2) decrease the maximum achievable lift coefficient, 3) enhance post-stall lift recovery, 4) increase the upwind vortex sheet size, and 5) decrease the size of the downwind vortex sheet.

For a given sideslip angle, sideforce slope increased with increasing angle of attack and then decreased. The decreasing tendency is attributed to merging of forward and aft panel vortices.

Wing-body configuration exhibited symmetric flow pattern and near-zero lateral-directional forces and moments at angles of attack prior to stall.

The wing exhibited large abrupt changes in rolling moment, yawing moment, and sideforce at the stall, even at zero sideslip angle. These effects are attributed to asymmetric vortex bursting.

Adding the body to the wing resulted in reduction in maximum achievable lift coefficient, a lower stall angle, and an increase in pitch stability.

Adding the body to the wing resulted in increased levels of adverse rolling and yawing moments at the stall. These effects are attributed to asymmetric vortex bursting and an increase in vortex spanwise spacing at prestall angles, observed in the wake surveys.

The wake surveys show that a narrow band at the edge of the vortex sheet has a very steep total pressure gradient present in all configurations. Interior gradients are not as steep.

Acknowledgment

The authors wish to express their gratitude to Dr. J. E. Lamar of NASA Langley Research Center for his arranging the balance and model loans and for his valuable advice.

References

1. Manor, D., "Low Aspect Ratio Wing/Body Vortex Interaction at Large Angles of Pitch and Yaw," Ph.D. Dissertation, Wichita State University, Wichita, Kansas, Jan. 1983.
2. Wentz, W. H. Jr., "Vortex Breakdown on Slender Sharp Edged Wings," Ph.D. Dissertation, University of Kansas, Lawrence, 1969.
3. Wentz, W. H. and McMahon, M. C., "An Experimental Investigation of the Flow Fields About Delta and Double-delta Wings at Low Speeds," NASA CR-521, 1966.
4. Wentz, W. H. and McMahon, M. C., "Further Experimental Investigations of Delta and Double-delta Wings at Low Speeds," NASA CR-714, 1967.
5. Lamar, J. E., "Prediction of Vortex Flow Characteristics of Wings at Subsonic and Supersonic Speeds," *Journal of Aircraft*, Vol. 13, July 1976.
6. Lamar, J. E., "Design Charts of Static and Rotary Stability Derivatives for Cropped Double-delta Wings in Subsonic Compressible Flow," NASA TN D-5661, 1970.
7. Staudacher, W., "Flugel mit kontrollierter Ablosung," Vortrag auf der 10. Jahrestagung der DGLR, Berlin, 1977, DGLR-Vorabdruck 77-028.
8. Lamar, J. E. and Luckring, J. M., "Recent Theoretical Developments and Experimental Studies Pertinent to Vortex Flow Aerodynamics—With a View Towards Design," *AGARD Conference Proceedings 247*, Jan. 1979, pp. 24-1 to 24-31.
9. Brennenstuhl, U. and Hummel, D., "On Vortex Formation Over Wings With Kinked Leading Edges," translated from "Untersuchungen Uber die Wirbelbildung an Flugeln mit Geknickten Vorderkanten," by David Manor, AR 82-9, Wichita State University, March 1982.
10. Wenlian, S., "An Experimental Investigation of Leading-Edge Spanwise Blowing," ICAS-82-6.6.4.
11. Brennenstuhl, U. and Hummel, D., "Vortex Formation Over Double-delta Wings," ICAS-82-6.6.5.
12. Lamar, J. E., "Analysis and Design of Strake-Wing Configurations," AIAA Paper 78-1201-R, 1978.
13. Ostowari, C., "An Experimental Investigation of Separated Three Dimensional Flow on General Aviation Twin-Engine Aircraft," Ph.D. Dissertation, Aerospace Engineering Department, Wichita State University, Wichita, Kan., Nov. 1982.
14. Crowder, J. P., "Quick and Easy Flowfield Surveys," *Astronautics and Aeronautics*, Oct. 1980.
15. Moore, W. A., "Effects of Forebody, Wing and Wing-Body-LEX Flow Fields on High Angle of Attack Aerodynamics," SAE Paper 791082, 1980.